sciendo

Slovak Journal of Civil Engineering

Vol. 27, 2019, No. 1, 14 – 24

DOI: 10.2478/sjce-2019-0003

COUPLING TANK MODEL AND LARS-WEATHER GENERATOR IN ASSESSMENTS OF THE IMPACTS OF CLIMATE CHANGE ON WATER RESOURCES

Naser MOHAMMADZADEH[1], Bahman Jabbarian AMIRI[1]*, Leila Eslami ENDERGOLI[2], Shirin KARIMI[1]

Abstract

With the aim of assessing the impact of climate change on surface water resources, a conceptual rainfall-runoff model (the tank model) was coupled with LARS-WG as a weather generator model. The downscaled daily rainfall, temperature, and evaporation from LARS-WG under various IPCC climate change scenarios were used to simulate the runoff through the calibrated Tank model. A catchment (4648 ha) located in the southern basin of the Caspian Sea was chosen for this research study. The results showed that this model has a reasonable predictive capability in simulating minimum and maximum temperatures at a level of 99%, rainfall at a level of 93%, and radiation at a level of 97% under various scenarios in agreement with the observed data. Moreover, the results of the rainfall-runoff model indicated an increase in the flow rate of about 108% under the A1B scenario, 101% under the A2 scenario, and 93% under the B1 scenario over the 30-year time period of the discharge prediction.

Address

[1] Dept. of Environmental Science, University of Tehran, Karaj, Iran

[2] Griffith University, Griffith School of Environment, Nathan Campus, Queensland, Australia

* ***Corresponding author:*** jabbarian@ut.ac.ir

Key words

- Climate change,
- Impact,
- Downscaling,
- Rainfall-Runoff model,
- LARS-WG,
- Tank model.

1 INTRODUCTION

The Earth's climate is increasingly changing over recent years (Vijaya Venkata Raman et al., 2012), and climate change and its consequences have become one of the greatest human challenges (Jain and Kumar, 2012; Salehi and Zebardast, 2016). During the last decade, several studies on economic growth have predicted the impact of climate change on some of the important dimensions of human welfare such as agriculture (Kang et al., 2009; Long et al., 2004), industry (Haq et al., 2011; Qian et al., 2011; Steinfeld et al., 2006), human health (Barrett et al., 2015; De Blois et al., 2015), energy demands, and economic growth. Due to the close relationship between climatic factors and plant growth (Hatfield et al., 2011), studies in that field have exclusively been focused on agriculture (Hatfield and Prueger, 2015; Koluman and Silanikove, 2014). The majority of these studies have investigated the consequences of changes in temperature and precipitation and failed to account for changes in other climatic variables such as moisture, wind speed, sunshine duration, and evaporation, which can have significant impacts on the availability of water resources as a key element in natural ecosystems and human life.

The IPCC's Fifth Assessment Report (AR5) clearly highlights the numerous negative impacts of the recent climate change on life-supporting systems in general and physical and biological systems in particular (Pachauri et al., 2014). Predictions based on general circulation models (GCMs) suggest an increase in the amount and quantity of large climatic events as well as changes in precipitation patterns across the world (Molanezhad, 2017). Accordingly, climate change could alter precipitation and evaporation patterns and affect available water resources both temporally and spatially. It is noteworthy that most of the research undertaken in assessing the environment have not taken climate change policies into account (Moss et al., 2010; Nakicenovic et al., 2000).

During the last decade, considerable work has been undertaken on the hydrological impacts of climate change world-wide (Islam

et al., 2014). In this case, hydrologists and water resource managers are most interested in evaluating the impact of climate change on the catchment-scale, as downscaling the models has remarkably enhanced our understanding of climatic behavior on smaller scales (Ghanghermeh et al., 2017). Hence, the number of studies evaluating the effect of climate change on the catchment-scale is increasing (Masood and Takeuchi, 2016). An assessment of the impact of climate change on snow hydrology in the Fraser River basin, Canada, has indicated that the extent of the snow distribution is projected to shrink by 20% (Islam et al., 2017).

The intensity and frequency of water shortages in the Yellow River basin, China, have been predicted to rise in the upcoming years (Wang et al., 2017). On the other hand, there is evidence indicating that climate change might cause increases in annual precipitation, which in turn could lead to increases in river flows, and maximum temperatures (Tan et al., 2017).

More importantly, it should be noted that climate change might cause significant changes in the amount and magnitude of floods. A study on the effects of climate change on water resources management indicated that climate change-induced increases in precipitation in the Meghna catchment had a great impact on the number of flood events in northeast Bangladesh (Masood and Takeuchi, 2016).

Coupling hydrology-climate change is mostly conducted by linking a process-based hydrological model with one of the most frequently used downscaling models, which include but are not limited to LARS-WG and SDSM. Dibike and Coulibaly (2005) applied LARS-WG and SDSM in a linkage with two hydrological models (HBV-96 and Canadian SEQUEAU) to investigate the hydrological impacts of climate change in the Saguenay catchment, Quebec, Canada, and found increasing trends in the mean temperature and precipitation and consequently an increase in the mean discharges of the basin.

According to studies conducted on the impact of climate change on water resources, it was determined that due to continuing climate change, water crises could be an integral part of human and other life forms. Hence, estimating water resources should be fully integrated in national planning, development, and management of water resources (Beyene et al., 2010).

To the best of the authors' knowledge, although there are a considerable number of studies in which spatially-explicit hydrological models have been applied as a dominant component in coupling with the output of weather generators, the authors believe that a gap exists in applying conceptual rainfall-runoff models within the framework of the coupling of hydrology-climatic models. Therefore, the present study has been designed and implemented to assess to what extent a conceptual rainfall-runoff model, namely the tank model, could be used to predict the impact of climate change on water resources.

2 MATERIAL AND METHODS

2.1 Study area

The study area is a catchment located in the southern basin of the Caspian Sea, where it has a high degree of significance due to its variety of natural landscapes and biodiversity (Nouri et al., 2008). It was selected by determining the correlation coefficient between the rainfall and river discharges in order to achieve a desirable level of performance during a rainfall-runoff modeling task involving 59 catchments. The highest correlation coefficient between the two parameters was observed in the Talarsar catchment. This catchment, with an area of 46.36 square km, consists of agriculture (1.5%), rangeland (0.07%), and forests (98.62) as land use/land cover classes. Figure 1 shows the geographical location of the Talarsar catchment in the southern basin of the Caspian Sea.

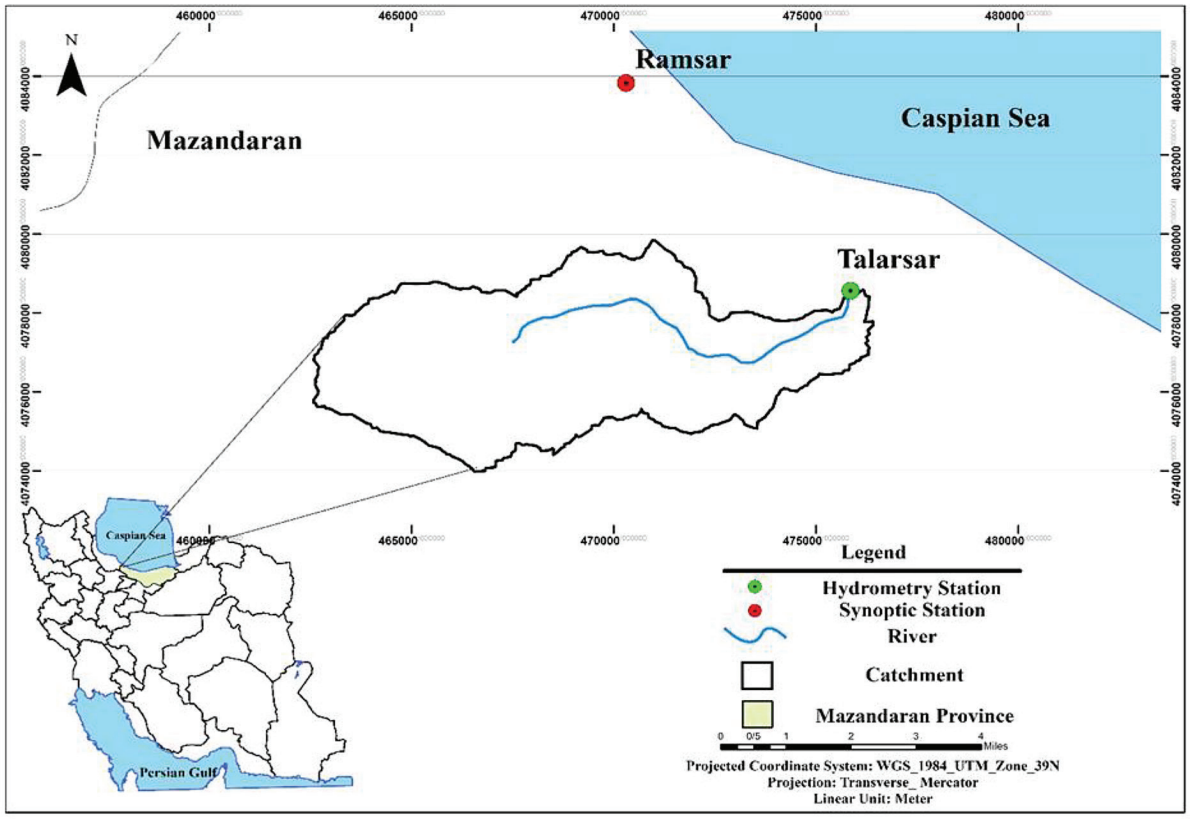

Fig. 1 *Location of the Talarsar catchment in the southern basin of the Caspian Sea*

2.2 Data sets

The daily mean discharge (m^3/s) data were obtained from the Iran Water Resources Management Authority. The maximum and minimum air temperature, rainfall (mm/day), solar radiation (MJ/m^2), and sunshine duration (hour/day) were obtained from the Ramsar meteorological station. A digital elevation model (DEM) and land use/land cover map were acquired from the USGS website and the Iran Forests and Rangelands Organization, respectively.

2.3 Methods

Figure 2 depicts the methodological flow diagram of the different steps undertaken in conducting the present study. Accordingly, these steps are briefly described in the following sub-sections below:

2.3.1 Statistical downscaling of the climatic data

The statistical downscaling of the climatic data was conducted by applying the LARS-WG, which was mainly due to its advantages in relation to other models (Semenov et al., 1998). It contains a series of statistical downscaling models that have improved the spatial accuracy of GCMs and, due to its time and cost-effectiveness, has widely been favored by users (Semenov et al., 1998). Moreover, the LARS-WG has a higher temporal, spatial and economic degree of superiority than dynamic downscaling models do (Wilks and Wilby, 1999). LARS-WG generates a relatively long daily time series of weather data with implications for hydrological assessments or agriculture. These daily climatic variables are considered to be the largest inputs to hydrological, agricultural and land use models; therefore, the appropriate length of time helps in estimating the probability of future extreme events (Semenov et al., 1998). The LARS-WG has successfully been implemented in many previous studies around the world (e.g., Semenov et al., 1998; Qian et al., 2004; Babaeian and Kwon, 2005; Lawless and Semenov, 2005, and Khan et al., 2006). It should be noted that statistical downscaling models have a degree of accuracy and computational speed than other models do that are applied to predict climatic parameters (Fujihara et al., 2008).

Using the observed climatic data (rainfall, sunshine duration, maximum, and minimum temperatures) for the time period of 1996-2010 as inputs to the statistical downscaling LARS-WG model, the projections of future climatic data (including rainfall, solar radiation, and minimum and maximum temperatures) of HADCM3 (the Hadley Centre coupled model) were downscaled for the period of 2020-2050. The scenarios considered are: A_1B (assumes very rapid economic growth for the upcoming period), A_2 (assumes regional economic development for the upcoming period), and B_1 (assumes environmentally sustainable development for the upcoming period).

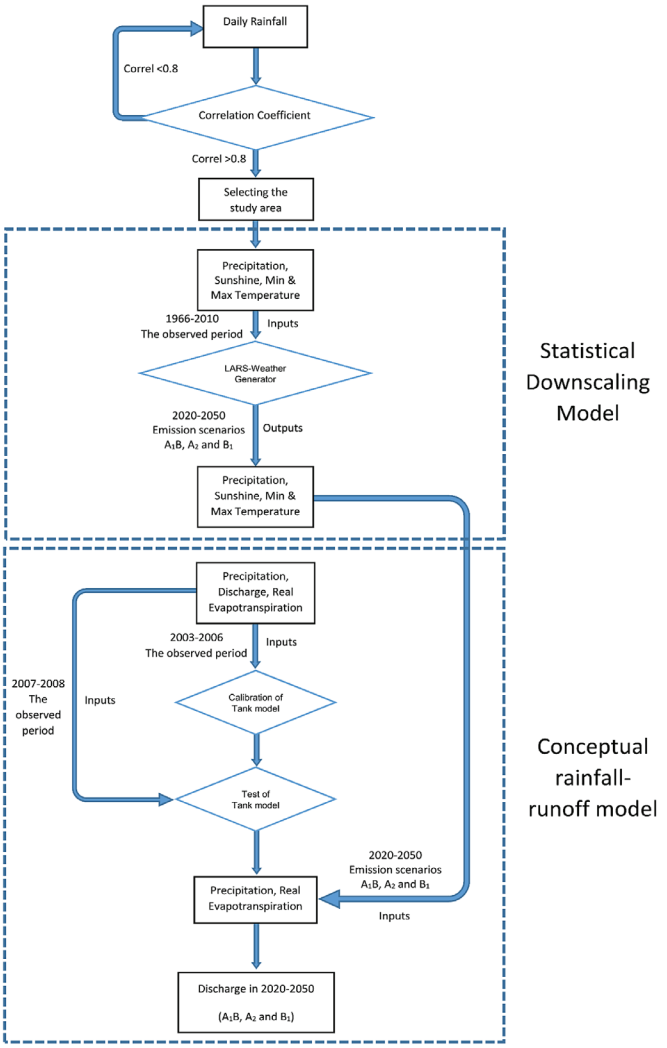

Fig. 2 *The coupling steps of the tank model and the LARS-WG in the present study*

2.3.1.1 Validation of the Lars-Weather Generator

The validation of a model is a process which determines how well the model's predictions are consistent with reality (Jørgensen and Bendoricchio, 2001) and the degree to which the model gives the users a realistic description of the real world. Therefore, in this study, which aims at assessing the reliability of the LARS-WG downscaling model, absolute linear evaluation metrics have been applied. It should be noted that O_i are the observed values, and P_i stands for the predicted values in Eqs. 1-5.

i. Absolute Maximum Error

The Absolute Maximum Error metric (AME) (Eq.-1), which is based on actual units, indicates the magnitude of the worst possible positive and negative errors that the model may produce. The numerical value of this measure is non-negative and has no upper bound (Dawson et al, 2007).

$$AME = \max(|O_i - P_i|) \quad (1)$$

ii. Peak Difference:

The Peak Difference metric (PDIFF) (Eq.-2), which is based on actual units, indicates to what extent the greatest value among the modelled datasets matches the largest recorded value of the observed data set. The numeric value has no upper bound (Dawson et al., 2007).

$$PDIFF = \max(O_i) - \max(P_i) \quad (2)$$

iii. Mean Absolute Error:

The Mean Absolute Error metric (MAE) (Eq.-3) was proposed by Schafer in the 1980s (Mayer and Butler, 1993) in order to indicate the degree of consistency between observed and modelled datasets based on actual units. The numerical value of this measure is non-negative and has no upper bound (Dawson et al., 2007).

$$MAE = \frac{1}{n}\sum_{i=1}^{n}|O_i - P_i| \quad (3)$$

iv. Mean Error:

The Mean Error metric (ME) (Eq.-4), which is based on actual units, illustrates the level of overall agreement between the observed and modelled datasets. This metric has no upper bound (Dawson et al., 2007).

$$MAE = \frac{1}{n}\sum_{i=1}^{n}(O_i - P_i) \tag{4}$$

v. Root Mean Squared Error

The Root Mean Squared Error metric (RMSE) (Eq.-5) was introduced by Picard and Cook in 1984 (Mayer and Butler, 1993) to indicate in actual units the level of overall agreement between observed and modelled datasets (Dawson et al., 2007).

$$RMSE = \sqrt{\sum_{i=1}^{n}\frac{(O_i - P_i)^2}{n}} \tag{5}$$

2.3.2 Tank model

The conceptual rainfall-runoff Tank model has been widely used in studies worldwide (Tingsanchali, 2001, Elhassan et al., 2001) to determine the relationship between rainfall and runoff. The tank model is considered to be a catchment-based model (Amiri et al., 2016). It is a simple model consisting of several tanks vertically connected in a series (Sugawara et al., 1984). A standard tank consists of 4 vertically and 5 horizontally-oriented reservoirs (Setiawan et al., 2003). Figure 3 illustrates the sections of a standard tank and the parameters and water regime for a given catchment. The various sections of the tank model from top to bottom are the Surface Reservoir (A), Intermediate Reservoir (B), Sub-base Reservoir (C) and Base Reservoir (D). The base reservoir can be filled by water, and if evapotranspiration dominates, this trend can be reversed (Setiawan et al., 2003). The outlets reflecting the outflow are Surface Flow (Ya2), Subsurface Flow (Ya1), Intermediate Flow (Yb1), Sub-base Flow (Yc1), and Base Flow (Yd1). Each outflow only shows the water level at each reservoir (Ha, Hb, Hc and Hd) that is higher than its outlet (Ha1, Ha2, Hb1 and Hc1). Moreover, the outflow at each outlet is affected by the outlet characteristics, including A0, A1, A2, B0, B1, C0, C1, and D1, which are also known as the parameters of the tank model (Setiawan et al., 2003).

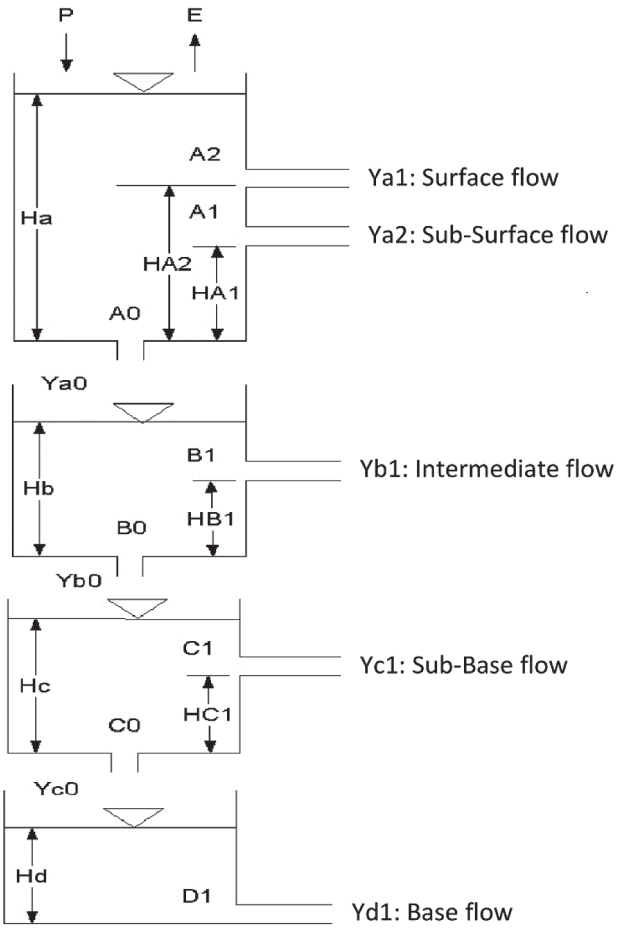

Fig. 3 *Illustration of the sections of a standard tank model and the parameters and water regime for a given catchment (Adapted from Sugawara et al., 1984 and Amiri et al., 2015)*

The parameters of the tank model can be categorized into two groups: 1) parameters reflecting hydrological processes (A_0, A_1, A_2, B_0, B_1, C_0, C_1, and D_1), and 2) parameters representing the water level (Ha_1, Ha_2, Hb_1 and Hc_1); each characteristic is assigned an initial value for each of the four reservoirs (Amiri et al., 2016).

According to the concept of the tank model, the base reservoir can be filled by water, and the horizontal outlet of each reservoir can show the flow rate of the outflow. The total outflow from the side outlets of the tanks can simulate the river flow rate (Sugawara et al., 1984):

$$\frac{dH}{dt} = P_{(t)} - ET_{(t)} - Y_{(t)} \tag{6}$$

Where

H	height of water (mm/day)
P	depth of rainfall (mm/day)
ET	evapotranspiration (mm/day)
Y	total flow (mm y-1)
t	time (day)

In the tank model, the total flow is estimated by adding the vertical flows of all the tanks as follows:

$$Y(t) = Ya(t) + Yb(t) + Yc(t) + Yd(y) \tag{7}$$

where Ya(t), Yb(t), Yc(t) and Yd(t) are vertical flows of each of the four tanks from top to bottom (Figure 2). The water balance for each tank is calculated using the following equations:

$$\frac{dH_a}{dt} = P(t) - Et(t) - Ya(t) \tag{8}$$

$$\frac{dH_b}{dt} = Ya_0(t) - Yb(t) \tag{9}$$

$$\frac{dH_c}{dt} = Yb_0(t) - Yc(t) \tag{10}$$

$$\frac{dH_d}{dt} = Yc_0(t) - Yd(t) \tag{11}$$

where Y_a, Y_b, Y_c and Y_d represent the vertical flow components of tanks A, B, C, and D, respectively. Ya_0, Yb_0 and Yc_0 show the horizontal flow components of tanks A, B, and C, respectively (Amiri et al., 2016). The total outflow (y) is defined as the flow resulting from the accumulation of the outflows of a water system in a given area. Hence, the total outflow (y) is the target for evaluating the performance of the tank model (Setiawan et al., 2003).

A set of input data is required to calibrate the tank model, including the daily mean river flow rate (mm/day), daily rainfall (mm/day), and actual evapotranspiration (Ev) (mm/day). Ev was calculated using the Hargreaves equation (Amiri et al., 2016):

$$ET_0 = 0.0135(T + 17.78)R_S \tag{12}$$

where ET_0 is the potential evapotranspiration (mm/day); Rs is the evaporation equivalent to solar radiation (mm/day), which is used to

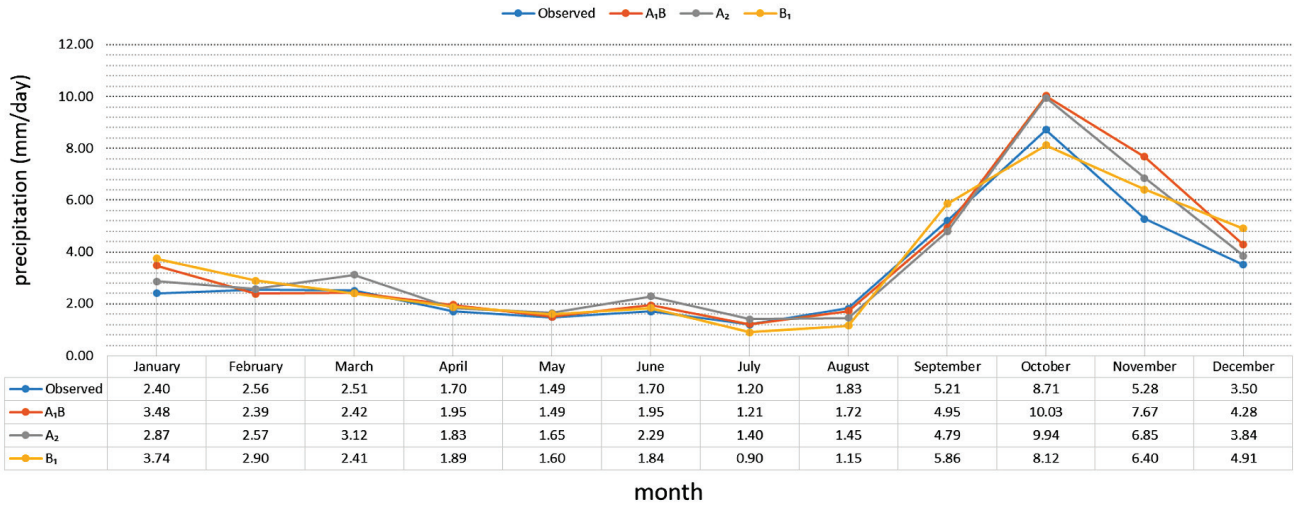

	January	February	March	April	May	June	July	August	September	October	November	December
Observed	2.40	2.56	2.51	1.70	1.49	1.70	1.20	1.83	5.21	8.71	5.28	3.50
A_1B	3.48	2.39	2.42	1.95	1.49	1.95	1.21	1.72	4.95	10.03	7.67	4.28
A_2	2.87	2.57	3.12	1.83	1.65	2.29	1.40	1.45	4.79	9.94	6.85	3.84
B_1	3.74	2.90	2.41	1.89	1.60	1.84	0.90	1.15	5.86	8.12	6.40	4.91

Fig. 4 *Comparison of the observed and predicted precipitation under the A_1B, A_2 and B_1 scenarios*

estimate the duration of sunshine (Allen et al., 1998); and T is the mean temperature (centigrade) for estimating actual evapotranspiration. ET_0 needs to be changed using the following equation (Amiri et al., 2016).

$$E_v = K_c \times ET_0 \tag{13}$$

where Ev is the actual evapotranspiration (mm/day), and K_c is the crop coefficient or land use. It should be noted that the measure of Kc is influenced by crop type, climate, soil, and crop growth stage. For example, the measure of Kc for wetlands that are located in a temperate climate with short vegetation is 1.10, while the Kc of open water (water depth < 2 m and water depth > 5 m) are 1.05 and 0.65, respectively (Allen et al., 1998).

The Tank model optimizer program (Yanto and Setiawan 2003; Setiawan et al. 2003) was utilized to optimize the model parameters. The Nash-Sutcliffe efficiency index (Eq. 14) was used to evaluate the performance of the optimization model for each catchment. This index ranges between 1 and ∞.

$$EI = \frac{\sum_{t=1}^{t}(Q_0^t - Q_m^t)^2}{\sum_{t=1}^{t}(Q_0^t - \overline{Q_0})^2} - 1 \tag{14}$$

where Q_o is the observed discharge (m^3/s), and Q_m is the predicted discharge (m^3/s) and the mean observed discharge (m^3/s). It should be noted that if EI is equal to 1, the observed and predicted values are in perfect agreement, while if EI is equal to 0, the model has no predictive ability (Amiri et al., 2016).

3 RESULTS

3.1 The outputs of the LARS-Weather Generator

The daily mean precipitation and maximum and minimum temperature data of the catchment under study were used as the model inputs. Due to the lack of the sunshine duration data, radiation data were introduced into the LARS-WG model. Changes in the mean precipitation, maximum, and minimum temperatures, and radiation were simulated under the A_1B, A_2 and B_1 emission scenarios for the 2020-2050 period. The absolute linear evaluation metrics (including AME, PDIFF, MAE, ME, and RMSE) were used in order to validate the downscaled model (Amiri, 2017).

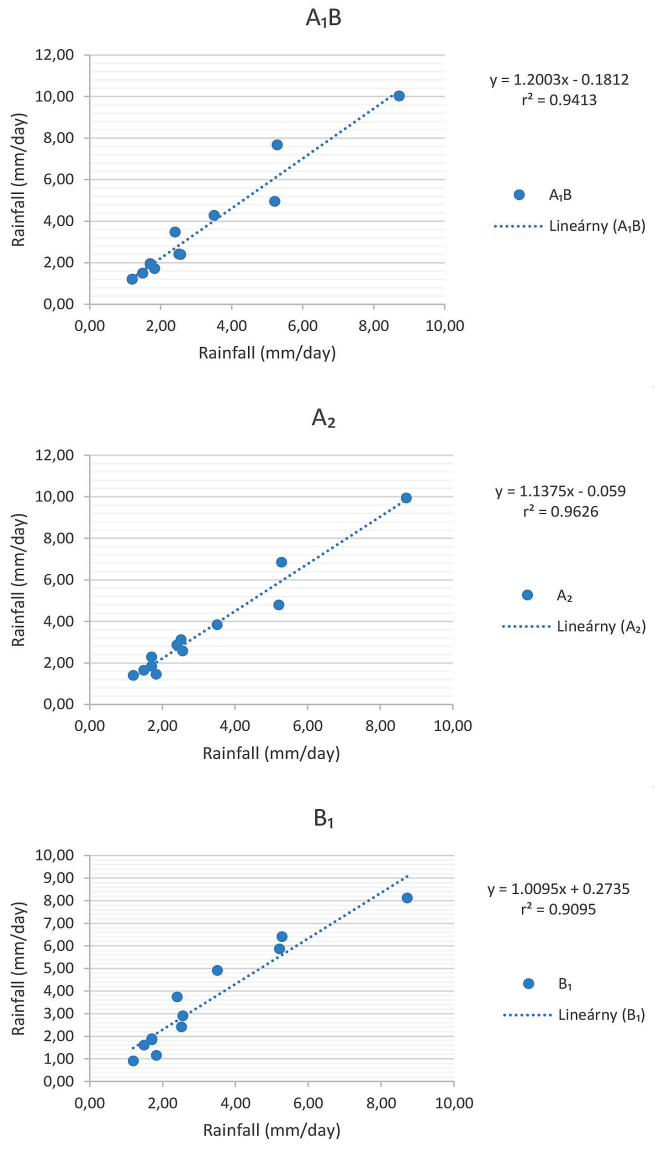

Fig. 5 *Observed versus predicted rainfall under the A_1B, A_2 and B_1 scenarios*

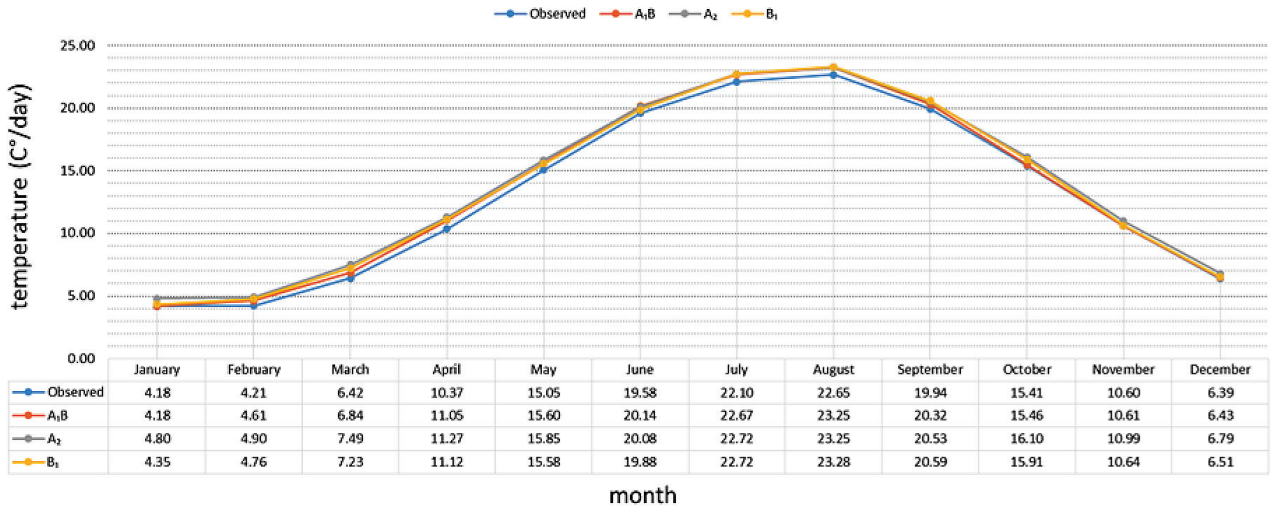

	January	February	March	April	May	June	July	August	September	October	November	December
Observed	4.18	4.21	6.42	10.37	15.05	19.58	22.10	22.65	19.94	15.41	10.60	6.39
A_1B	4.18	4.61	6.84	11.05	15.60	20.14	22.67	23.25	20.32	15.46	10.61	6.43
A_2	4.80	4.90	7.49	11.27	15.85	20.08	22.72	23.25	20.53	16.10	10.99	6.79
B_1	4.35	4.76	7.23	11.12	15.58	19.88	22.72	23.28	20.59	15.91	10.64	6.51

Fig. 6 *Observed versus predicted temperature under the A1B, A2 and B1 scenarios*

3.1.1 Downscaling the precipitation

The average simulated precipitation under scenarios A_1B, A_2, and B_1 increased by 11.44%, 11.64%, and 8.15%, respectively, in comparison to the observation period based on the LARS-WG model (Fig. 4). The observed *versus* the simulated data under different scenarios is depicted in Figure 5. The validation results of the LARS-WG model, based on the above-mentioned models for the simulated precipitation, are presented in Table 1.

Tab. 1 *Results of the validation of the LARS-WG model for different climatic variables*

Climatic variable	The Metrics of the Model's Validation				
	RMSE	ME	MAE	PDIFF	AME
Rainfall	19.48	-0.46	6.09	-33.9	6.09
Min. temperature	3.23	-0.35	2.51	-0.8	2.51
Max. temperature	5.37	0.14	4.17	0.1	4.17
Sunshine duration	3.84	-0.56	2.89	3.00	2.89

3.1.2 Downscaling the minimum temperature

On average, the expected minimum temperature under the A_1B, A_2, and B_1 scenarios increased by 3.13, 7.28, and 4.71 degrees Celsius (°C) respectively in comparison to the observation period based on the LARS-WG model (Fig. 6). Fig. 7 indicates the relationship between the observed and simulated data under the different scenarios. Table 1 presents the results of the LARS-WG model validation for the simulated precipitation.

3.1.3 Downscaling the maximum temperature

On average, the maximum predicted temperature under the A_1B, A_2, and B_1 scenarios increased by 2.86, 4.85, and 3.68 °Celsius (°C) respectively in comparison to the observation period based on the LARS-WG model (Fig. 8). Figure 9 and Table 1 present the scatter points of the observed and simulated data under the different scenarios and the results of the LARS-WG model validation for the simulated precipitation, respectively.

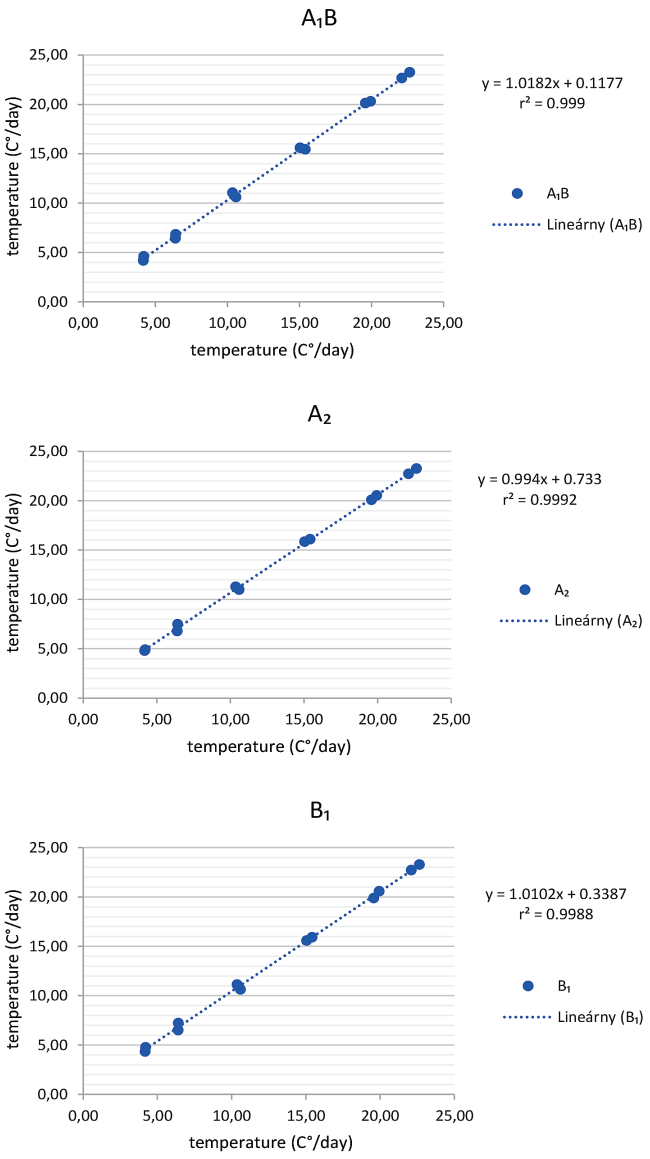

Fig. 7 *Observed versus predicted temperature under the A_1B, A_2 and B_1 scenarios*

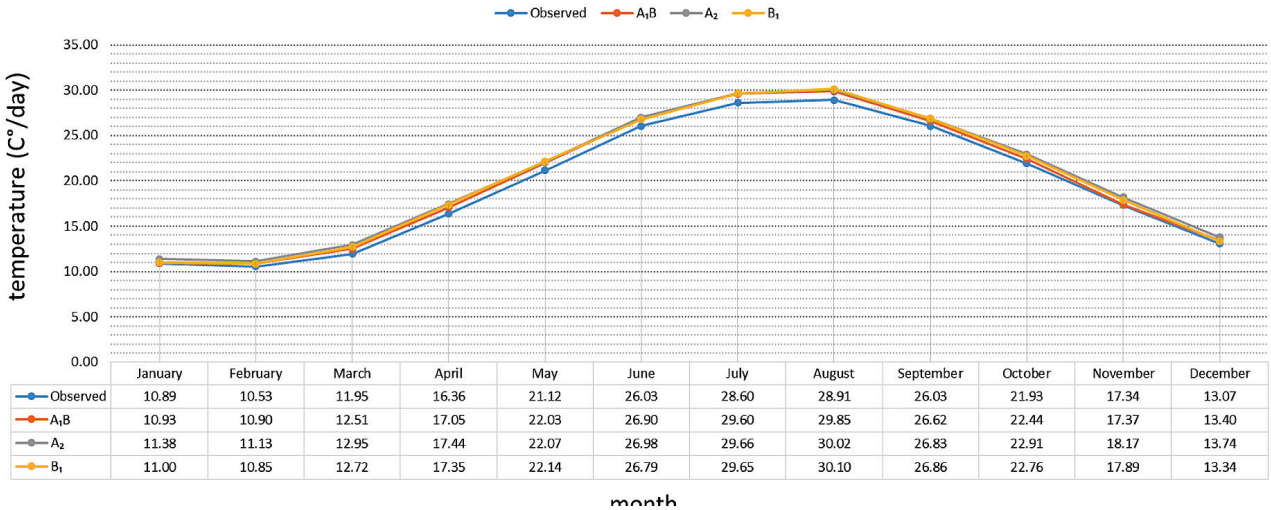

	January	February	March	April	May	June	July	August	September	October	November	December
Observed	10.89	10.53	11.95	16.36	21.12	26.03	28.60	28.91	26.03	21.93	17.34	13.07
A_1B	10.93	10.90	12.51	17.05	22.03	26.90	29.60	29.85	26.62	22.44	17.37	13.40
A_2	11.38	11.13	12.95	17.44	22.07	26.98	29.66	30.02	26.83	22.91	18.17	13.74
B_1	11.00	10.85	12.72	17.35	22.14	26.79	29.65	30.10	26.86	22.76	17.89	13.34

Fig. 8 *Comparison of the maximum observed and predicted temperatures under the different scenarios*

3.1.4 Downscaling the sunshine radiation

Based on the LARS-WG model, the simulated radiation under the A_1B, A_2, and B_1 scenarios increased on average by 4.8%, 3.9%, and 4.5% respectively in comparison to the observation period (Fig. 10). Fig. 11 shows the observed versus simulated measures under the different scenarios. The validation results of the LARS-WG model based on the above-mentioned models for simulated precipitation are indicated in Table 1.

3.2 Coupling of the Tank model and LARS-Weather Generator

The tank model should be calibrated and tested before coupling it with the LARS-WG. The observed water flow data from 2003 to 2008 (6 years) was used for the calibration, and it was used from 2007 to 2008 (2 years) for testing the model. The Nash-Sutcliffe efficiency index (NSEI) value resulting from the calibration of the tank model was 0.83, which indicates the predictive ability of the model. NSEI values closer to 1 indicates a higher agreement between the observed and simulated values, while lower values (closer to 0) indicate that the model has a low predictive ability. Therefore, given the fact that the resulting value is close to 1, the model can be used for predicting the future.

Following the tank model's calibration, data from the statistical testing period were introduced to the model and, according to the calibration, the model generated the discharge data for the testing period. Figure 12 shows the hydrograph of the tank model for the statistical testing period.

Due to the fact that the LARS-WG downscaling model will be used to generate the climatic parameters for the period of 2020-2050, the predicted precipitation data at the Ramsar Station were introduced to the tank model to simulate the water flow. Table 5 shows the monthly mean flow rate and the percentage increase in the simulated monthly mean flow rate relative to the observed values. Figure 13 compares the observed and simulated monthly mean flow rates.

According to the various scenarios, the precipitation in the catchment is projected to increase by 11.5% under the A_1B scenario and 8% under the A_2 scenario over the simulation period. Therefore, according to these results, the mean predicted flow rate is projected to increase by 104% under the A_1B and A_2 scenarios and by 88% under the B_1 scenario relative to the observation period.

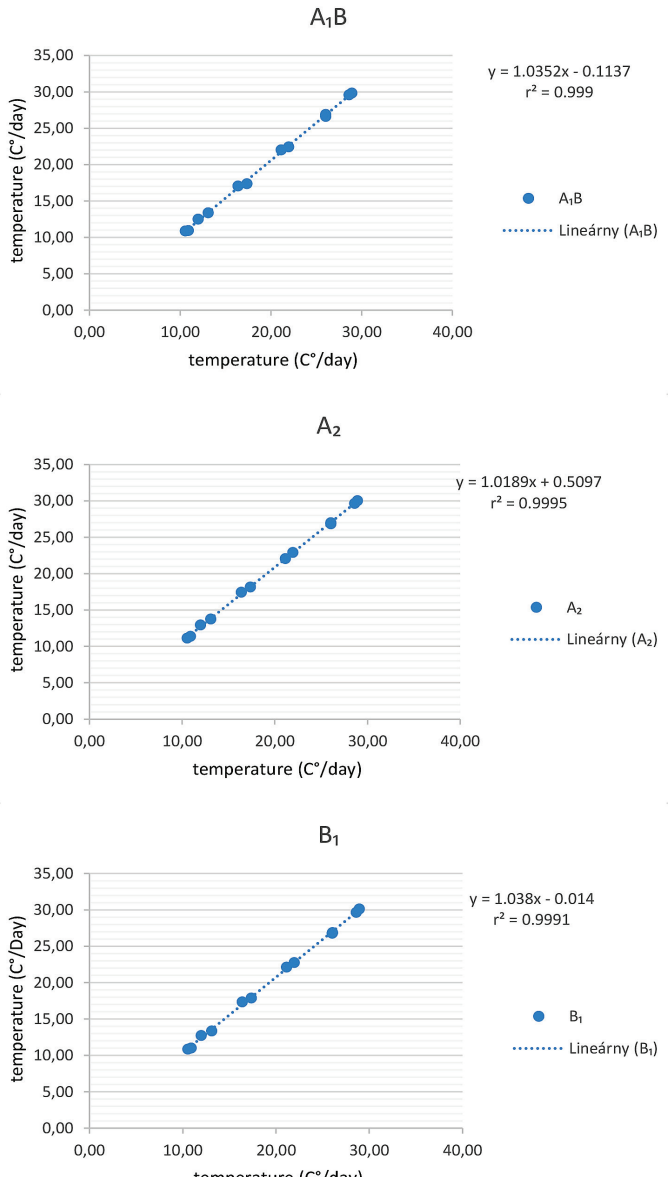

Fig. 9 *Observed versus predicted maximum temperature under the A_1B, A_2 an B_1 scenarios*

	January	February	March	April	May	June	July	August	September	October	November	December
Observed	3.10	3.21	2.97	3.78	4.77	5.59	5.45	4.84	3.93	3.69	3.28	2.94
A_1B	2.58	3.11	2.64	3.73	4.59	5.95	5.65	4.80	3.54	3.47	3.12	2.66
A_2	2.93	2.99	2.44	3.77	4.54	5.79	5.68	5.02	3.50	3.33	3.38	2.80
B_1	2.67	2.93	2.48	3.71	4.87	5.99	5.86	4.99	3.37	3.46	3.28	2.59

Fig. 10 *Comparison of the observed and predicted solar radiation under the A_1B, A_2 and B_1 scenarios*

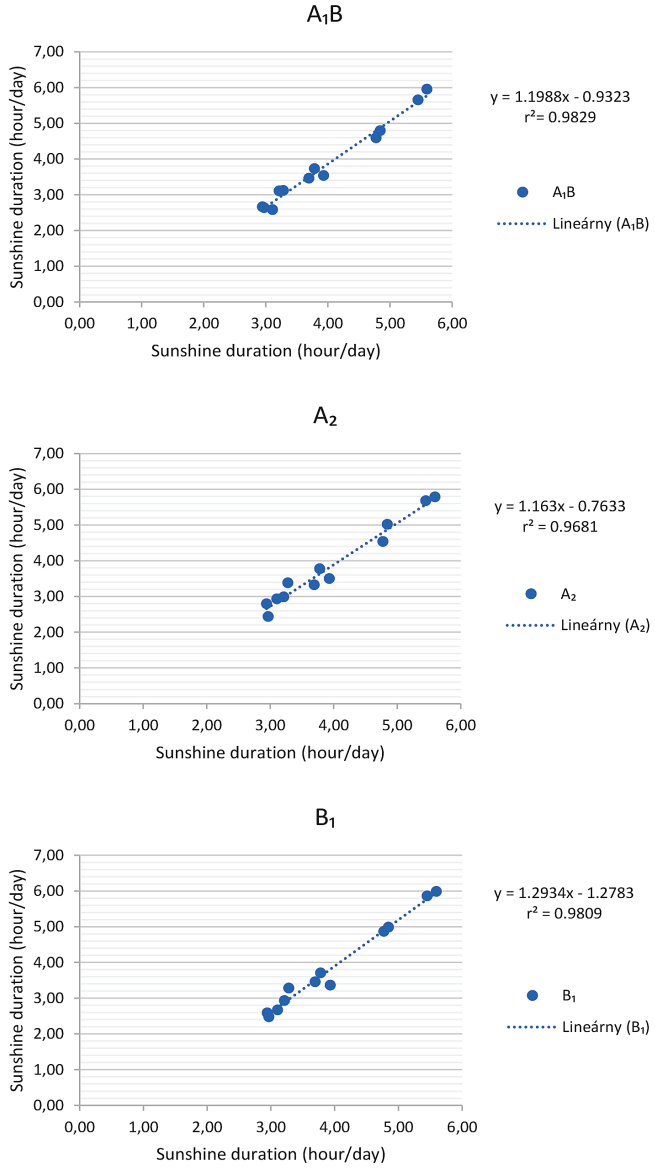

Fig. 11 *Observed versus predicted sunshine duration under the A1B, A2 and B1 scenarios*

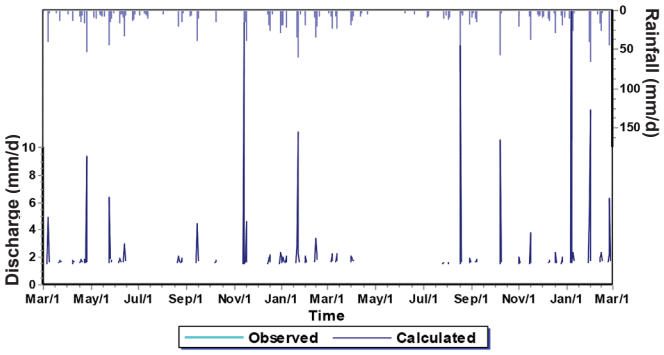

Fig. 12 *Hydrograph of the Tank model for the test period*

4 CONCLUSION

Applying the general circulation model (GCM) through the weighting method leads to a reduction in uncertainty and, as a result, a more accurate estimation of the effects of climate change on the temperature and rainfall, as well as the runoff and flooding in the catchment. In order to cope with the limitations of the GCM model, such as spatial resolution, downscaling is one of the key aspects of climate change impact studies. In the present study, the LARS-WG model was used for downscaling the rainfall and the minimum, maximum, and radiation data. Since the LARS-WG model estimates future data such as the temperature, rainfall, and radiation by appropriately distributing parameters, it can provide more accurate results. In this study, the potential impact of climate change on the surface water resources in the Talarsar catchment was investigated over a 30-year period (2020-2050). The statistical downscaling LARS-WG model under the A_1B, A_2 and B_1 climate change scenarios was used to downscale some weather parameters such as precipitation, radiation, and the minimum and maximum temperatures. On the other hand, the conceptual tank model was used to simulate the flow rate. The results of the LARS-WG showed that precipitation is projected to slightly decrease in the summer time, but significantly increase in other seasons. Moreover, the radiation will experience a slight increase in the summer and a slight decrease in all the other seasons. The minimum and maximum temperatures in the observation period showed a slight increase. The results of the downscaling model are consistent with

those of other studies, thus indicating the acceptable performance of the modeling procedures. Moreover, the results from the tank model showed increasing flow rates of about 108%, 101% and 93% under the A_1B, A_2, and B_1 scenarios. Hence, it is essential to find a suitable way to mitigate the adverse effects of climate change on flow rates and adopt proper decisions about increasing flow rates in the future.

Tab. 5 *Monthly mean flow rate and the percentage increase in the simulated monthly mean flow rate relative to the observed values*

Month	Obs. Discharge	A_1B scenario		A_2 scenario		B_1 scenario	
		Sim. Discharge	Change (%)	Sim. Discharge	Change (%)	Sim. Discharge	Change (%)
January	0.60	1.44	140.00	1.42	136.67	1.48	146.67
February	0.84	1.36	61.90	1.37	63.10	1.38	64.29
March	0.47	1.35	187.23	1.36	189.36	1.29	174.47
April	0.73	1.33	82.19	1.30	78.08	1.24	69.86
May	0.63	1.31	107.94	1.25	98.41	1.20	90.48
June	0.90	1.36	51.11	1.27	41.11	1.15	27.78
July	0.68	1.30	91.18	1.17	72.06	1.08	58.82
August	0.56	1.30	132.14	1.16	107.14	1.07	91.07
September	0.79	1.87	136.71	1.60	102.53	1.60	102.53
October	0.84	2.10	150.00	2.27	170.24	1.94	130.95
November	1.02	1.81	77.45	1.84	80.39	1.78	74.51
December	0.89	1.56	75.28	1.56	75.28	1.69	89.89
Mean	0.75	1.51	107.76	1.46	101.20	1.41	93.44

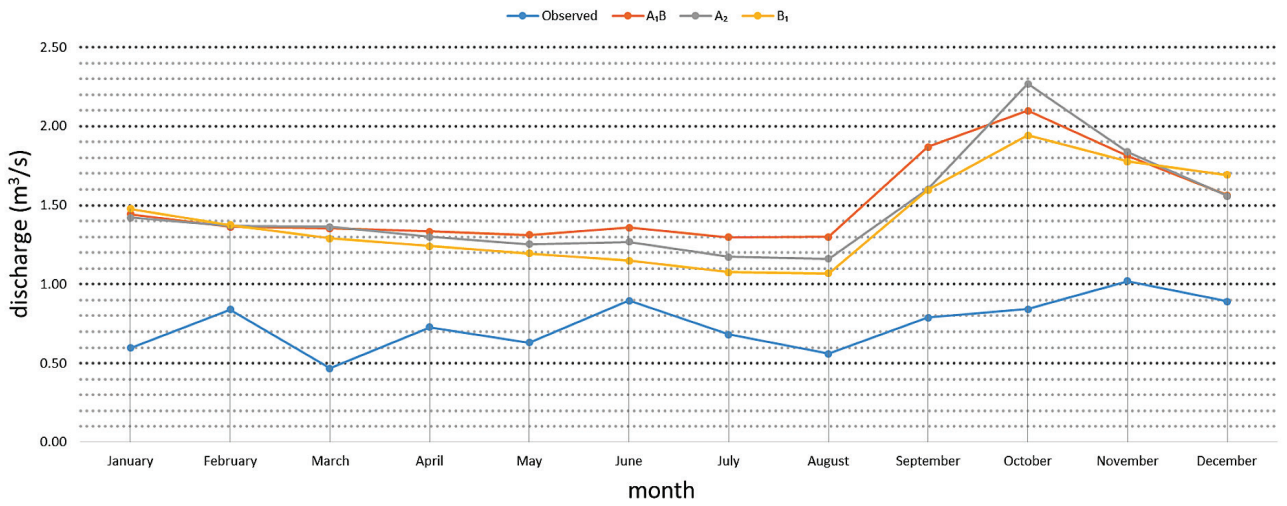

Fig. 13 *Comparison of the observed and simulated mean monthly flow under the different scenarios*

REFERENCES

Amiri, B. J. (2017) *Environmental Modeling*. University of Tehran Press, No. 3883, pp. 150.

Amiri, B. J., Fohrer, N., Cullmann, J., Hörmann, G., Müller, F., Adamowski, J. (2016) *Regionalization of Tank Model Using Landscape Metrics of Catchments*. Water resources management, 30(14), pp. 5065-5085.

Allen, R. G., Pereira, L. S., Raes, D., Smith, M. (1998) *Crop evapotranspiration - Guidelines for computing crop water requirements-FAO*. Irrigation and drainage paper 56. *FAO, Rome*, *300*(9), p. D05109.

Babaeian, I., Kwon, W. T. (2005) *Climate change assessment over Korea using stochastic daily data*. In Proceedings of the first Iran–Korea joint workshop on climate modelling.

Barrett, B., Charles, J. W., Temte, J. L. (2015) *Climate change, human health, and epidemiological transition*. Preventive medicine, 70, pp. 69-75.

Beyene, T., Lettenmaier, D. P., Kabat, P. (2010) *Hydrologic impacts of climate change on the Nile River Basin: implications of the 2007 IPCC scenarios*. Climatic change, 100(3-4), pp. 433-461.

Dibike, Y. B., Coulibaly, P. (2005) *Hydrologic impact of climate change in the Saguenay watershed: comparison of downscaling methods and hydrologic models*. Journal of hydrology, 307(1-4), pp. 145-163.

De Blois, J., Kjellstrom, T., Agewall, S., Ezekowitz, J.A., Armstrong, P.W., Atar, D. (2015) *The effects of climate change on cardiac health.* Cardiology, 131(4), pp. 209-217.

Dawson, C. W., Abrahart, R.J., See, L. M. (2007) *HydroTest: a web-based toolbox of evaluation metrics for the standardised assessment of hydrological forecasts*. Environmental Modelling & Software, 22(7), pp.1034-1052.

Elhassan, A. M., Goto, A., Mizutani, M. (2001) *Combining a tank model with a groundwater model for simulating regional groundwater flow in an alluvial fan*. Transactions of the Japanese Society of Irrigation, Drainage and Reclamation Engineering (Japan).

Fujihara, Y., Tanaka, K., Watanabe, T., Nagano, T., Kojiri, T. (2008) *Assessing the impacts of climate change on the water resources of the Seyhan River Basin in Turkey: Use of dynamically downscaled data for hydrologic simulations*. Journal of Hydrology, 353(1-2), pp. 33-48.

Ghanghermeh, A., Roshan, G., Nasrabadi, T. (2017) *Synoptic approach to forecasting and statistical downscaling of climate parameters (Case study: Golestan Province)*. Pollution, 3(3), pp. 487-504.

Haq, Z., Ishaq, M., Khan, M. (2011) *Economic growth and agrifood import perfor-mance of emerging economies and Next-11*. Afr. J. Bus. Manag, 5, pp. 10338-10344.

Hatfield, J. L., Boote, K. J., Kimball, B. A., Ziska, L. H., Izaurralde, R. C., Ort, D., Thomson, A. M., Wolfe, D. (2011) *Climate impacts on agriculture: implications for crop production.* Agronomy Journal, *103*(2), pp. 351-370.

Hatfield, J. L., Prueger, J. H. (2015) *Temperature extremes: Effect on plant growth and development*. Weather and climate extremes, 10, pp. 4-10.

Islam, S. U., Déry, S. J., Werner, A. T. (2017) *Future climate change impacts on snow and water resources of the Fraser River Basin, British Columbia*. Journal of Hydrometeorology, 18(2), pp. 473-496.

Islam, S., Bari, M., Anwar, F. (2014) *Hydrologic impact of climate change on Murray–Hotham catchment of Western Australia: a projection of rainfall–runoff for future water resources planning*. Hydrology and Earth System Sciences, 18(9), pp. 3591-3614.

Jørgensen, S. E., Bendoricchio, G. (2001) *Fundamentals of ecological modelling* (Vol. 21). Elsevier.

Jain, S. K., Kumar, V. (2012) *Trend analysis of rainfall and temperature data for India*. Current Science, pp. 37-49.

Kang, Y., Khan, S., Ma, X. (2009) *Climate change impacts on crop yield, crop water productivity and food security–A review*. Progress in Natural Science, 19(12), pp. 1665-1674.

Koluman, N., Silanikove, N. (2014) *Impacts of climate change on the goat farming sector in harsh environments*. Small Rumin. doi, 10.

Khan, M. S., Coulibaly, P., Dibike, Y. (2006) *Uncertainty analysis of statistical downscaling methods*. Journal of Hydrology, 319(1-4), pp. 357-382.

Lawless, C., Semenov, M. A. (2005) *Assessing lead-time for predicting wheat growth using a crop simulation model*. Agricultural and forest meteorology, 135(1-4), pp. 302-313.

Long, S. P., Ainsworth, E. A., Rogers, A., Ort, D.R. (2004) *Rising atmospheric carbon dioxide: plants FACE the future*. Annu. Rev. Plant Biol., 55, pp. 591-628.

Masood, M., Takeuchi, K. (2016) Climate change impacts and its implications on future water resource management in the Meghna Basin. *Futures*, *78*, pp. 1-18.

Moss, R. H., Edmonds, J. A., Hibbard, K. A., Manning, M. R., Rose, S. K., Van Vuuren, D. P., Carter, T. R., Emori, S., Kainuma, M., Kram, T., Meehl, G. A. (2010) *The next generation of scenarios for climate change research and assessment*. Nature, 463(7282), p. 747.

Mayer, D. G., Butler, D. G. (1993) *Statistical validation*. Ecological modelling, 68(1-2), pp. 21-32.

Molanezhad, M. (2017) *Statistical modeling of the association between pervasive precipitation anomalies in Southern Alburz and global ocean-atmospheric patterns.* Pollution, 3(1), pp. 167-174.

Nakicenovic, N., Alcamo, J., Grubler, A., Riahi, K., Roehrl, R. A., Rogner, H. H., Victor, N. (2000) *Special report on emissions scenarios (SRES), a special report of Working Group III of the Intergovernmental Panel on Climate Change*. Cambridge University Press.

Nouri, J., Karbassi, A. R., Mirkia, S. (2008) *Environmental management of coastal regions in the Caspian Sea*. International Journal of Environmental Science & Technology, 5(1), pp. 43-52.

Pachauri, R. K., Allen, M. R., Barros, V. R., Broome, J., Cramer, W., Christ, R., Church, J. A., Clarke, L., Dahe, Q., Dasgupta, P., Dubash, N. K. (2014) *Climate change 2014: synthesis report. Contribution of Working Groups I, II and III to the Fifth*

Assessment Report of the Intergovernmental Panel on Climate Change (p. 151). IPCC.

Qian, B., Gameda, S., Hayhoe, H., De Jong, R., Bootsma, A. (2004) *Comparison of LARS-WG and AAFC-WG stochastic weather generators for diverse Canadian climates*. Climate Research, 26(3), pp. 175-191.

Qian, G., Guo, X., Guo, J., Wu, J. (2011) *China's dairy crisis: impacts, causes and policy implications for a sustainable dairy industry*. International Journal of Sustainable Development & World Ecology, 18(5), pp. 434-441.

Setiawan, B. I., Fukuda, T., Nakano, Y. (2003) *Developing procedures for optimization of Tank Model's Parameters*. Agricultural Engineering International: CIGR Journal.

Semenov, M. A., Brooks, R. J., Barrow, E. M. Richardson, C. W. (1998) *Comparison of the WGEN and LARS-WG stochastic weather generators for diverse climates*. Climate research, 10(2), pp. 95-107.

Steinfeld, H., Gerber, P., Wassenaar, T. D., Castel, V., Rosales, M., Rosales, M., de Haan, C. (2006) *Livestock's long shadow: environmental issues and options*. Food and Agriculture Organization.

Sugawara, M., Watanabe, I., Ozaki, E., Katsugama, Y. (1984) *Tank model with snow component.* Research Notes of the National Research Center for Disaster Prevention No. 65. *Science and Technolgoy, Ibaraki-Ken, Japan.*

Semenov, M. A., Barrow, E. M., Lars-Wg, A. (2002) *A stochastic weather generator for use in climate impact studies*. User Man Herts UK.

Salehi, E., Zabardast, L. (2016) *Application of Driving Force-Pressure-State-Impact-Response (DPSIR) framework for integrated environmental assessment of the climate change in city of Tehran*. Pollution, 2(1), pp. 83-92.

Tan, M. L., Yusop, Z., Chua, V. P., Chan, N. W. (2017) *Climate change impacts under CMIP5 RCP scenarios on water resources of the Kelantan River Basin, Malaysia*. Atmospheric Research, 189, pp. 1-10.

Tingsanchali, T. (2001) *Application of combined Tank Model and AR Model in flood forecasting.* In 4th DHI Software Conference, Helsingor, Denmark. Available at: http://www. dhisoftware. com/uc2001/Abstracts_Proceedings/Papers01/057/057. htm (accessed May 2005).

Vijaya Venkata Raman, S., Iniyan, S., Goic, R. (2012) *A review of climate change, mitigation and adaptation*. Renewable and Sustainable Energy Reviews, 16(1), pp. 878-897.

Wang, G., Zhang, J., Jin, J., Weinberg, J., Bao, Z., Liu, C., Liu, Y., Yan, X., Song, X., Zhai, R. (2017) *Impacts of climate change on water resources in the Yellow River basin and identification of global adaptation strategies*. Mitigation and adaptation strategies for global change, 22(1), pp. 67-83.

Wilks, D. S., Wilby, R. L. (1999) *The weather generation game: a review of stochastic weather models*. Progress in physical geography, 23(3), pp. 329-357.

Yanto R., Setiawan B. I. (2003) *Optimization of tank model using genetic algorithm.* Department of Agricultural Engineering, IPB, Bogor, Indonesia. Accessed 27 Feb 2013 from http://web.ipb.ac.id/~budindra/